

# 1B.6 THREE DIMENSIONAL STRUCTURE OF EASTERLY WAVE DISTURBANCES OVER AFRICA AND THE TROPICAL NORTH ATLANTIC

George N. Kiladis\* and Chris D. Thorncroft\*\*

\*NOAA Aeronomy Laboratory, Boulder, Colorado

\*\*Department of Earth and Atmospheric Sciences, SUNY Albany, NY

## 1. Introduction

Recent studies of the structure of African easterly waves (AEWs) have indicated that these disturbances occur over a broad range of time scales and can have distinctly different dynamical structures depending on their location with respect to the low level African easterly jet (AEJ, Pytharoulis and Thorncroft, 1995). Westward moving disturbances having quasi-periodicities of roughly 3-5 day and 6-9 days are dominant (Diedhiou et al., 1999), and other lower frequency modes with around 10-15 and 25-60 day periods have been observed as well (Janicot and Sultan, 2001). This study aims to provide a comprehensive statistical view of the structure of AEWs and the dynamics governing their behavior.

## 2. Data and Methodology

We utilize a variety of data sources, including the Outgoing Longwave Radiation (OLR) data set to categorize deep convective rainfall, ECMWF and NCEP/NCAR reanalyses, and radiosonde data from several long-term stations. The reanalysis data are daily averages at 2.5° resolution. We also use the high resolution CLOUD Archive User Service (CLAUS) brightness temperature data set, which has 8 times daily data at .5° spatial resolution.

Easterly wave activity can be readily isolated through space-time filtering of the OLR or CLAUS data following the methodology of Wheeler and Kiladis (1999). In that study a so-called "TD-type" signal was identified as a pronounced spectral peak in global OLR during the northern summer months for westward propagating wavenumbers greater than six and for periods between 2-6 days. Here we filter for this wavenumber-frequency band and use the resulting OLR field as a predictor in a linear regression model. We note that the results are quite insensitive to the details of this filtering, as long as it includes variability at around 4 days, since AEWs with this time scale are a dominant signal during the monsoon.

TD-filtered OLR for the June-September season was used as an independent variable in the regression model at a variety of base grid points over Africa. Here we show spatial patterns from ECMWF reanalysis, for which the 1979-93 period was available. A longer record (1979-2001) was available for the NCEP/NCAR and sonde data, and results are very consistent among these various data sets. A regression relationship between wind, temperature, geopotential height and humidity is calculated at each global grid point versus the TD-filtered OLR at the base point. In the case of sonde data, the OLR grid point closest to the station was used as the predictor. All fields shown are scaled to a typical OLR perturbation of  $-20 \text{ W/m}^2$ .

## 3. Results

Fig. 1 shows the OLR and 850 hPa streamfunction and statistically significant wind fields associated with TD OLR at the point 10°N, 10°W over West Africa. Plots shown are for two days prior to the peak of convection (Day-2, top), Day 0 (middle), and Day+2 (bottom). In this sequence the OLR signal propagates westward at a phase speed of around 12 m/s, typical of AEWs on the equatorward side of the AEJ. The period of this disturbance, as measured from regressed CLAUS data (not shown), is close to 3.5 days.

The circulation associated with the wave shows an interesting evolution with respect to the location of the convection through the sequence. On Day-2 when the main convective center is located to the east of the Greenwich meridian and the wave is amplifying, the convection is located in northerly flow at 850 hPa, to the west (ahead) of the low level trough. As the wave moves closer to the coast and convection peaks on Day 0, the trough is then nearly coincident with the convective center, and once convection moves offshore on Day+2 it becomes embedded in the southerly flow to the east of (behind) the trough as in a classical oceanic easterly wave. This phase shift occurs because the wavetrain moves westward faster than the convective center itself, a result confirmed by Hovmueller diagrams of the  $v$  component of the wind.

Vertical cross sections of circulation fields of the wave from reanalysis data (not shown), reveal that they tilt strongly eastward with height when they are east of Greenwich, have a more or less "first baroclinic" tropospheric structure with opposite-signed stacked in the vertical over West Africa, then develop westward tilts with height over the Atlantic. This occurs essentially because the lower level perturbations propagate faster than those at upper levels, which have a peak amplitude at around 200 hPa.

Signals during the passage of an AEW in the Dakar sonde record (located at 14.7°N, 17.5°W) are shown in Fig. 2. An eastward tilted structure of the  $v$  wind with height is seen below 300 hPa, with an opposite tilt above that level. While convection is peaking at Day 0 there is southerly flow at low levels, consistent with the structure of Fig. 1c. Peak southerly flow occurs at around 700 hPa on Day+1 and at 200 hPa on Day-1. Upper tropospheric temperature (Fig. 2b) shares the same tilt (westward with height) as the  $v$  wind but down to 500 hPa, with an opposite sign below that having little if any tilt. The lower troposphere is cool (warm) in southerlies (northerlies), consistent with the mean low level temperature gradient. The variability of the upper tropospheric temperature peaks at 300 hPa, and is likely a combination of the effects of latent heating, advection, and a dynamical wave response.

\*Correspondence: George N. Kiladis, R/AL3, 325 Broadway, Boulder CO 80305 [kgiladis@al.noaa.gov](mailto:kgiladis@al.noaa.gov)

#### 4. Discussion

The observed changes vertical structure as AEWs propagate westward imply a fundamental change in their energetics. Over Africa, lower tropospheric eastward tilts with height (i.e. against the vertical shear of the AEJ) are consistent with baroclinic growth (e.g. Thorncroft and Hoskins, 1994) while to the west the opposite tilt implies more important contributions by barotropic energy conversions and possibly convection. This interpretation is also consistent with the change in horizontal tilt in Fig. 1, from northwest-southeast to southwest-northeast south of the axis of the AEJ, which in the mean runs between 10°-15°N at 600 hPa over West Africa (Diedhiou et al., 1999).

#### 5. References

Diedhiou, A., S. Janicot, A. Viltard, P. de Felice, and H. Laurent, 1999: Easterly wave regimes and associated convection over West Africa and tropical Atlantic: results from the NCEP/NCAR and ECMWF reanalysis. *Climate Dynamics*, **15**, 795-822.

Janicot, S., and B. Sultan, 2001: Intra-seasonal modulation of convection in the West African monsoon. *Geophys. Res. Lett.*, **28**, 523-526.

Pytharoulis, I, and C. Thorncroft, 1999: The low-level structure of African easterly waves in 1995. *Mon. Wea. Rev.*, **127**, 2266-2280.

Thorncroft, C., and B.J. Hoskins, 1994: An idealized study of African easterly waves. I: A linear view. *Quart. J. Roy. Met. Soc.*, **120**, 953-982.

Wheeler, M., and G.N. Kiladis, 1999: Convectively coupled equatorial waves: Analysis of clouds and temperature in the wavenumber-frequency domain. *J. Atmos. Sci.*, **56**, 374-399.

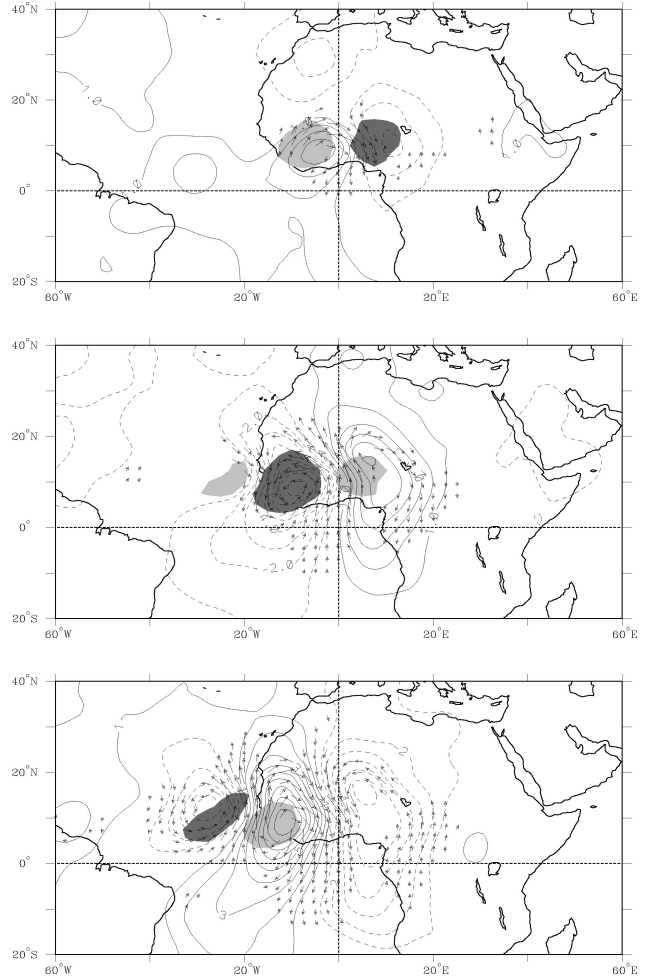


Fig. 1. Regressed OLR (dark shading negative), significant wind, and streamfunction (contours) at 850 hPa associated with negative TD-filtered OLR perturbations at 10°N, 10°W. a) Day-2 (top), b) Day 0 (middle), and c) Day+2 (bottom).

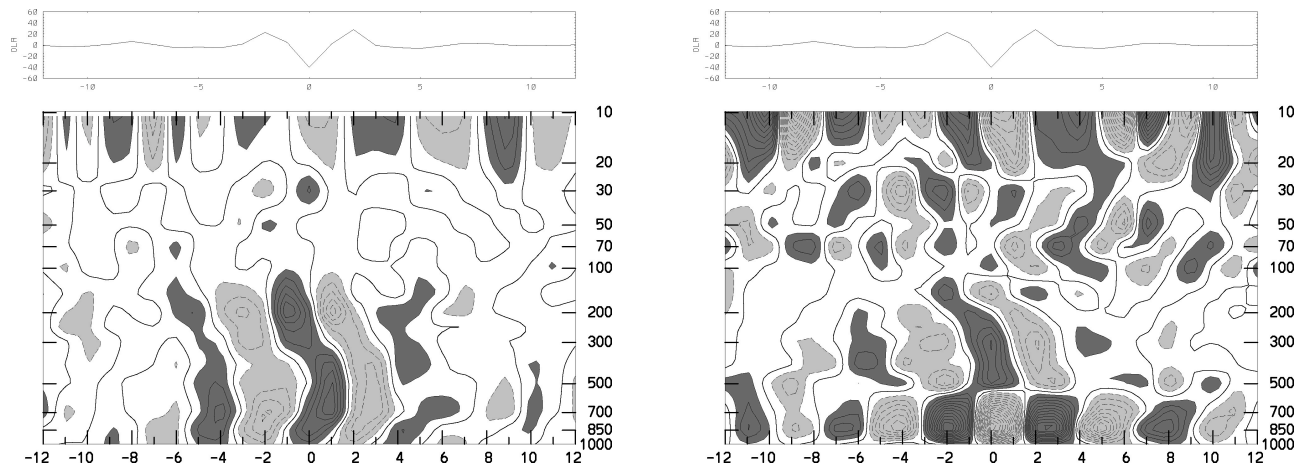


Fig. 2. Regressed  $v$  (left, a) and temperature (right, b) at Dakar from Day-12 through Day+12 and from 1000 hPa up to 10 hPa based on the passage of a  $-20 \text{ W/m}^2$  TD-filtered OLR perturbation on Day 0. Contour interval is  $.5 \text{ m/s}$  for wind (dark shading southerly) and  $.1^\circ\text{C}$  for temperature (dark shading positive). Time series of OLR perturbation at the grid point nearest to Dakar is shown along the top.